Sheffield Hallam University

B-site vacancy induced Raman scattering in BaTiO3-based ferroelectric ceramics

VEERAPANDIYAN, Vignaswaran K., SAMAN KHOSRAVI, H., CANU, Giovanna, FETEIRA, Antonio <http://orcid.org/0000-0001-8151-7009>, BUSCAGLIA, Vincenzo, REICHMANN, Klaus and DELUCA, Marco

Available from Sheffield Hallam University Research Archive (SHURA) at:

http://shura.shu.ac.uk/26361/

This document is the author deposited version. You are advised to consult the publisher's version if you wish to cite from it.

Published version

Copyright and re-use policy

Sheffield Hallam University Research Archive
http://shura.shu.ac.uk

Short communication

B-site vacancy induced Raman scattering in BaTiO$_3$-based ferroelectric ceramics

Vignaswaran K. Veerapandiyan[a,*], Saman Khosravi H[b], Giovanna Canu[c], Antonio Feteira[d], Vincenzo Buscaglia[c], Klaus Reichmann[b], Marco Deluca[a,*]

[a] *Materials Center Leoben Forschung GmbH, Roseggerstrasse 12, 8700 Leoben, Austria*
[b] *Institute for Chemistry and Technology of Materials, Graz University of Technology, 8010 Graz, Austria*
[c] *CNR-ICMATE, Institute of Condensed Matter Chemistry and Technologies for Energy, National Research Council, Via de Marini 6, 16149, Genoa, Italy*
[d] *Materials Engineering and Research Institute, Sheffield Hallam University, Sheffield, S11WB, United Kingdom*

A B S T R A C T

Defects, in particular vacancies, play a crucial role in substituted perovskite systems, influencing the structural features that underpin ferroelectricity. B-site vacancies introduce cation disorder in the perovskite lattice and are in fact one of the main driving forces for relaxor behaviour in barium titanate (BaTiO$_3$, BT) based ferroelectrics. In this work, material systems are carefully selected to qualitatively study the change in B-site vacancy concentration for heterovalent substituted BT-based ferroelectric polycrystals. Raman spectroscopy was used to investigate those systems, and B-site vacancy specific Raman modes were identified unambiguously by comparison with charge-compensated BT, where B-site vacancies are absent. This study validates the hypothesis that vacancies induce Raman scattering because of symmetry breaking in the BT lattice, establishing this method as a vital tool to study substitutional defects in ceramic materials.

1. Introduction

Barium titanate (BaTiO$_3$, BT), a prototypical room-temperature ferroelectric (FE) material with ABO$_3$ perovskite form, undergoes a sequence of structural phase transitions before entering into the paraelectric phase above the Curie temperature (125 °C) [1]. Ferroelectricity in BT is due to the long-range correlation of Ti (B-site) cation displacements and can be modulated by chemical modification upon substitution of alternative chemical species in the equivalent perovskite lattice sites. This has been a common scientific practice to explore the possibilities of finding better performing material systems [2–6], and is an opportunity to tune material properties such as the polarization response, loss mechanisms, electro-mechanical responses, Curie temperature, temperature stability of the permittivity, among others [7–9].

For BT-based ferroelectric systems, B-site substitution either with homo- or heterovalent cations results first in a characteristic evolution from FE behaviour to diffuse phase transition (DPT) behaviour before entering relaxor state for high substituent contents [10,11]. The onset of relaxor behaviour occurs for lower substituent contents in heterovalent substituted systems, compared to homovalent ones [12,13]. The structural or chemical origin of this difference is not yet fully understood, although the strong local fields determined by the effective

charge of the heterovalent dopant and the necessary charge-compensating defect are likely to play a major role [14]. Especially in heterovalent systems, vacancies (A-, B-site or oxygen) are expected to play a decisive role as charge compensating defects inducing disorder and modifying the functional properties [15].

Raman spectroscopy has been used often in the past to study ferroelectric materials, especially since – having a coherence length as low as a few nanometres [16] – it can access structural features not visible in laboratory X-ray [11,17,18]. For example, the coexistence of displacive and order-disorder components in BT were first reported from high temperature Raman spectra [19]. For any crystal structure, there is a specific number of Raman active modes that follows the selection rules (purely displacive) and the appearance of broad, disorder-related higher-order components that exist also in (first-order Raman forbidden) centrosymmetric phases at high temperature (above Curie temperature). In addition, there are additional Raman modes in defective or chemically modified systems because of symmetry breaking induced locally by the defects [20]. We show here that these aspects make Raman spectroscopy a useful tool to detect B-site vacancies and their change with composition.

In this work, we identify the Raman modes that are related to B-site defects in BT-based materials. B-site Nb^{5+} modified BT (BNbT) and A-

site La^{3+} modified BT (BLaT) are investigated since they are expected to bear B-site Ti^{4+} vacancies (even though substitution occurs at different sites). The results are then compared to B-site (Ga^{3+}-Nb^{5+}) co-substituted ceramic samples (BGaNbT) in which the vacancy concentration is expected to be drastically reduced by self-compensation preserving the charge neutrality in the lattice. In other words, we present here a way to qualitatively study the defects in perovskites, which constitutes a relevant input for the design of BT perovskite solid solutions with desired properties.

2. Experimental procedures

$BaTiO_3$, $Ba[Ti_{1-5x/4}Nb_x]O_3$, $[Ba_{(1-x)}La_x]Ti_{1-x/4}O_3$ and $Ba[(Ga_xNb_x)Ti_{(1-2x)}O_3]$ ceramics were fabricated by the conventional solid-state mixed oxide route. Based on the required chemistry, stoichiometric amounts of pure $BaCO_3$ (Electronic grade purity, Solvay Bario e Derivati, Italy; SSA = 3.3 m^2/g, electronic grade), TiO_2 (Electronic grade purity, Toho, Japan; SSA = 6.1 m^2/g, electronic grade), Nb_2O_5 (99.9% purity, H.C. Starck, SSA = 6.3 m^2/g, ceramic grade), La_2O_3 (+99%, Treibacher Industrie AG, Treibach, Austria) and Ga_2O_3 (99.99% purity, Aldrich Chemical Co., Milwaukee, WI) were weighed and ball milled using suitable solvent and grinding media for homogenous mixing. In case of BNbT and BLaT, where charge compensation is needed, Ti deficiency was taken in to account to avail the formation of Ti vacancies (V_{Ti}'''', in Kroger-Vink notation). After calcination and subsequent milling, the powders were compacted, pressed and sintered at different temperatures depending on the composition. Organic binders were used before pressing green ceramic bodies and a separate de-binding protocol was followed for the binder burn out process. Table 1 summarizes the compositional details of the investigated barium titanate based systems. Table S1 summarizes the processing parameters used to fabricate the investigated barium titanate based systems. Detailed reports on the fabrication of $Ba[(Ga_xNb_x)Ti_{(1-2x)}O_3]$ and $[Ba_{(1-x)}La_x]Ti_{1-x/4}O_3$ ceramics can as well be found in the literature [22,23].

Raman measurements were carried out in a LabRAM 300 spectrometer (Horiba Jobin Yvon, Villeneuve d'Ascq, France) using an excitation wavelength of λ = 532 nm in a backscattering geometry equipped with an edge filter (cut-off: 80 cm^{-1}), 1800 g/mm grating and CCD detector. The laser light was focused on the sample surface by means of a long working distance 100x objective (with NA 0.8, LMPlan FI, Olympus, Tokyo, Japan) and a spot size of 1 μm. The effective power at the sample surface was ~2 mW. Temperature-dependent Raman measurements were carried out in a Linkam (THMS600) temperature-controlled stage (Linkam, Tadworth, UK) placed under the Raman microscope. The spectra were visualized using commercial software environment (Origin 2018b, OriginLab Corp., Northampton MA, USA) after correcting for the Bose-Einstein population factor, and fitting was performed using Labspec 4.02 (Horiba Jobin Yvon) applying Gauss-Lorenz peak functions.

3. Results and discussion

In hard mode Raman spectroscopy, the phase transitions are usually studied by the change in vibrational energy of the crystal lattice that are evident in the observable phonons [18,24]. Fig. 1 shows the Raman
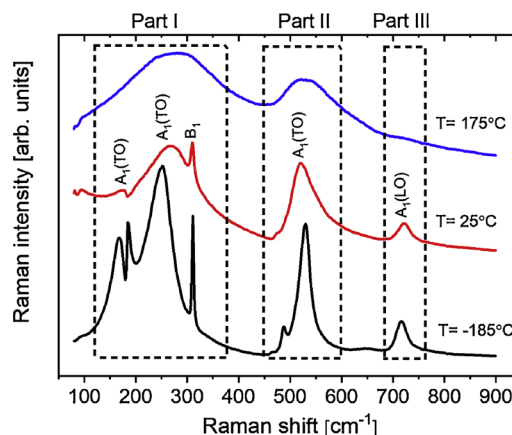

Fig. 1. Room temperature Raman spectra of pure BT at rhombohedral (−185 °C), tetragonal (25 °C) and cubic (175 °C) phases.

spectra of pure BT in the rhombohedral (−185 °C), tetragonal (25 °C) and cubic (175 °C) phases. The temperature dependent relative permittivity response of BT, showing also the same phase transitions, is reported for reference in Fig. S3. For tetragonal BT, Raman selection rules predict 13 first-order Raman modes from 100 cm^{-1} to 900 cm^{-1} [25]. In ceramics, however, unknown scattering geometries because of random grain orientation makes the mode assignment based on group theory not straightforward even when resolving peak convolutions using asymmetric peak shapes or polarised Raman measurements [26]. For this reason, only dominant modes within peak convolutions can be singled out, as highlighted in both Fig. 1 (BT) and Table 2. It is clear that the number of modes decreases with the increase in symmetry. Below the Curie temperature (125 °C), the spectrum can be divided into three parts. Modes associated with part I are related to the A-site and (from ~200 cm^{-1}) to B–O chains. In part II and part III, modes are associated to the vibration of oxygen atoms in the BO_6 octahedra of ABO_3 perovskite [27]. Based on the selection rules, a perfect (i.e. defect-free) perovskite lattice should have permissible modes only within these three zones in the energy landscape (cf. Table 2). Arguments related to selection rules hold validity for a defect-free perfect perovskite but are invalid when it comes to chemically modified systems because of a defective and discontinuous lattice [28]. Before discussing the Raman modes originated by defects in the perovskite lattice, there is one more aspect to consider, related to the structural phase transitions in these materials. In Fig. 1, above the T_c of BT, spectral features are visible, although theoretically any Raman activity should be forbidden in a cubic perovskite. These modes are due to second-order spectral components reflecting the phonon density of states, and are related to the intrinsic (dynamic) disorder of BT in the paraelectric phase above T_c [19,29].

When chemical modifications are introduced into the perovskite lattice, selection rules can be broken in addition to the dynamic disorder, both in the paraelectric and ferroelectric phases. Typical modifications appearing in the Raman spectrum in chemically substituted perovskites are the following:

1 Raman modes become broader with substitution concentration

Table 1
Compositional details of investigated barium titanate based systems.

Sample No	Sample name	Substitution site in BaTiO₃	Substitution concentration (at. %)	Oxidation number	Ionic radii (Å)
1	BNbT	Ti site	5	5+	0.64
2	BLaT	Ba site	5	3+	1.36
3	BGaNbT	Ti site	25 (Ga^{3+} + Nb^{5+})	Ga = 3+ & Nb = 5+ (4+ on average)	0.62 & 0.64

*Note: Ba^{2+} = 1.61 Å & Ti^{4+} = 0.605 Å.

Table 2

Dominant Raman modes that are observed in BT-based systems and extra modes that are categorized based on its origin.

Reference [20,26]		Present work			
	Symmetry	BT	BNbT	BLaT	BGaNbT
170	A1(TO)	175	183	197	–
270	A1(TO)	267	270	245	–
305	B1	309	300	–	–
520	A1(TO)	520	514	500	–
720	A1(LO)	720	723	727	–
Extra modes					
i-LVM		–	790	780	795
v-LVM		–	837	838	–
DARS		550 − 670	530 − 600	520 − 600	540 − 620

*Note: The position of Raman modes corresponds to the maximum of peak intensity. No Raman modes can be assigned with confidence for BGaNbT because of the severely disordered structure resulting from high substitution concentration. The wavenumber of extra modes are approximate values or ranges. All the wavenumbers are in cm^{-1}.

mainly as a result of structural disorder appearing upon substitution with ions of different valence state and/or ionic radii. In a continuous lattice, phonons are collective vibrations that can propagate throughout the whole lattice. This is not valid in substituted systems, where the intrinsic order is disrupted by chemical modification. This is the source of asymmetric broadening of Raman lines due to the collective confinement of phonons within symmetry-breaking regions. Studying the broadening in this case allows estimating the size of these regions [30].

2 Raman mode frequencies shift as a result of a change in bonding environments. In simple terms, a shift to higher frequencies of a Raman mode is the indication of a stronger chemical bond. In ferroelectric systems, this change in bonding environment is usually from substituents that carry a lone electron pair that facilitates orbital hybridization, ultimately resulting in a change in the bonding nature from prevalently ionic to covalent [26,31,32].

3 Appearance of extra Raman modes due to localised phonon vibrations in the vicinity of a (substitutional) defect, or as a result of the relaxation of Raman selection rules from defect-induced disorder [33].

Only the third aspect is addressed in this work. Extra Raman modes can be categorized widely into the following types [34]:

a Localized vibrational modes (LVM) that are normally seen above the optical branch because of chemical substitution with heavier atoms (*i*-LVM).

b Point defects such as vacancies inducing Raman modes similar to LVM (referred to as *v*-LVM).

c Modes resulting from the breaking of selection rules induced by disorder in chemically-modified systems. The mechanism is closely related to the phonon confinement described above (which is the source of asymmetric modes) and leads to the appearance of Raman bands at critical points in the Brillouin zone at which the phonon density of states is high (disorder-activated Raman scattering-DARS) [35].

In chemically modified BT, all the three types of extra Raman modes are demonstrated in this work using three sets of compositions along with pure BT (as described in Table 1). All the dominant Raman modes for the analysed compositions are summarized in Table 2. It is important to note that here all changes in peak positions are related to changes in the chemical environment and the associated atomic-level stresses. Peak shifts related to grain size effects in fact were not detected
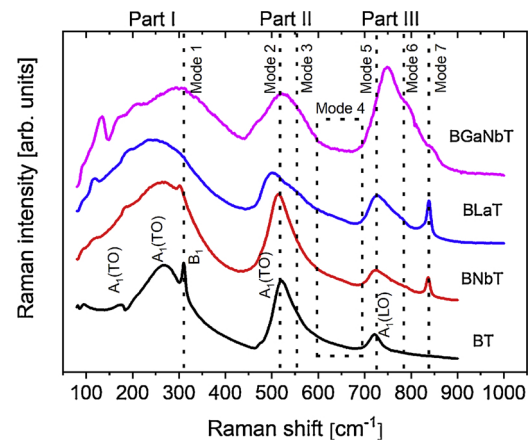
Fig. 2. Room temperature Raman spectra of chemically modified BT systems (cf. Table 2).

within the limits of our instrumentation, as evident from the good correspondence between Raman spectra of bulk and powdered BNbT and BLaT ceramics, as shown in Fig. S4. A detailed study of ceramic stresses in the present compounds is beyond the scope of this paper.

The charge compensation for BNbT and BLaT is achieved via V_{Ti}'''' [15,36] and this is valid from the processing point of view since all these samples were fabricated with Ti deficiency. The charge neutrality is preserved in BGaNbT and no vacancies are expected [11,37]. From Table 1, it is clear that the lattice continuum is broken upon substitution primarily by differences in the ionic radii and defects induced by difference in oxidation states compared to ions in the equivalent crystallographic sites. In this regard, the difference in the oxidation state and the charge compensation by formation of V_{Ti}'''' plays a vital role in BNbT. A very similar charge compensation occurs in BLaT but because of A-site chemical modification. However, in charge-compensated BGaNbT, we do not expect any effect from either point defects, different valence or ionic radii.

Because of chemical modification, several changes to the Raman spectra compared to pure BT are evident from Fig. 2. All the three groups of modes classified in prototypical BT (cf. Fig. 1) are evident in all compositions. In addition, it is important to note that mode 1, 2 and 5-present in all polar materials are the indicators of co-operative Ti^{4+} displacement in Ti–O chains, in other words, the ferroelectric nature of the material under test. BT and BNbT compositions are FE at RT. BLaT is weakly FE at RT since the Curie temperature is close to RT [21] and BGaNbT is a severely disordered dielectric material [22]. All the chemically modified BT-based systems are disordered as evident from the significant peak broadening (symmetric as well as asymmetric). These convolutions are likely a result of the chemical modification mentioned above. Mode 3 – appearing in both BT and substituted systems – is a DARS mode that is suggested to originate from lattice defects (such as oxygen vacancies), and thus is present also in pure BT (as evident from the asymmetric shape of the spectral convolution at $550 − 670$ cm^{-1}. Such DARS modes are more prominent near the modes that are associated to lighter ions (oxygen in case of BT), as is the case of mode 3 in Fig. 2. Interestingly, mode 3 is present also in the purest form of BT single crystals; Wada et al. [38] suggested that even pure BT possesses this type of disorder in its cubic phase, which agrees with the order-disorder model discussed earlier.

As evident from Fig. 2, also extra modes (Modes 4, 6 and 7) are visible in the substituted BT spectra. Minor unknown secondary phases were detected in BLaT and BGaNbT from the X-ray diffractogram (cf. Fig. S2, secondary phases marked with asterisks). These phases, however, do not impact the Raman signature and, consequently, extra modes are only related to heterovalent substitution. Raman peaks from secondary phases in fact appear sharp and will have an inconsistent

peak evolution during temperature dependent measurements since the probing spot is constantly changed due to thermal expansion of the samples (unlike for instance: Fig. S5). Table 2 summarizes all the categorized extra Raman modes that are observed in chemically modified BT based systems.

Mode 6 (cf. Fig. 2) is seen in all substituted systems, which suggests that it is activated by substitution, and not by the presence of vacancies. This mode is assigned as the asymmetric breathing of BO_6 and was previously related solely on the ionic radii mismatch caused by B-site substituents [18,39]. In particular, it was suggested that the shift of this mode is related to the ionic size mismatch between Ti and the foreign B-site substituent. Although ionic size mismatch may play a role in determining this mode's position, our results show that this is not the only responsible factor for the appearance of this mode. In BLaT, in fact, this mode appears although substitution is performed at the A-site and not at the B-site. From the work of Farhi et al. [24] and Pokorny et al. [20], it is clear that both in BNbT and BLaT, mode 6 evolves as a function of substitution concentration. We thus conclude here that mode 6 appears due to either the presence of a foreign atom or a Ti vacancy on the B-site. It is, in essence, due to the vibration of oxygens in perturbed octahedra (i.e. chemical pressure around the B-site). The presence of mode 6 in BGaNbT is associated with the absence of mode 1, which indicates that the material is not ferroelectric anymore but rather severely disordered. Mode 6 is thus assigned as an *i*-LVM mode. Note that BGaNbT did not show any FE behaviour in the measured temperature range of [−190 °C, 500 °C] whereas the BNbT and BLaT samples are FE below RT.

Mode 4 ('a hump') – as marked in the dotted box in Fig. 2 – is seen in all substituted systems except in BGaNbT. Mode 7, on the other hand, is seen in all substituted systems. Interestingly, this mode is very sharp in BNbT and BLaT, whereas in BGaNbT it is merely a broad shoulder. This may suggest a different origin of this mode in the substituted systems, specifically a defect-related origin only in BNbT and BLaT. BNbT and BLaT, in fact, were selected to replicate the same charge compensation mechanism although caused by a different chemical environment (i.e. B- and A-site substitution, respectively), to check if the occurrence of extra Raman modes due to B-site vacancies is consistent. BGaNbT was selected as control means (due to the absence of Ti vacancies), so that B-site vacancy modes (i.e. as type *v*-LVM modes) can be assigned. From this, it is clear (cf. Fig. 2) that both mode 4 (the hump) and mode 7 (sharp) are only observed in the samples that have significant vacancies in the system and are completely absent at all temperatures in dipole-pair substituted systems (BGaNbT) and in pure BT. These modes can be thus unequivocally assigned as *v*-LVM modes. In addition, it is important to note that the shoulder that is clearly recorded in BaGaNbT cannot be associated to a vacancy mode because of its peculiar T-dependent evolution. As can clearly be seen in Fig. S5, the intensity of the shoulder in BGaNbT decreases with increasing T, whereas the intensity of the sharp mode 7 stays constant at all temperatures in BNbT. The disappearance of this shoulder in BGaNbT clearly indicates the first-order nature of this Raman mode, which can likely be assigned as a *i*-LVM type mode resulting from the severe heterogeneity at the B-site (25% substitution in total). On the other hand, mode 7 in BNbT is T-independent, and its FWHM even decreases with increasing temperature (cf. Fig. S6), hence showing an opposite behaviour compared to the shoulder in BGaNbT. This behaviour of mode 7 in BNbT and BLaT is typical of a localised mode, which can be assigned to the presence of B-site (Ti) vacancies (*v*-LVM). Similar cases were shown previously by Tenne et al. for oxygen vacancies in the $SrTiO_3$ system [33,40], and suggest BO_6 breathing as vibration scheme.

The ratio of the relative intensities of mode 7 and mode 5 is presented for BNbT series with different Nb concentration along with BLaT for reference purposes (cf. Fig. 3). The microstructural information and RT relative permittivity of the BNbT sample series is provided in Table S2 for reference. For more information on the macroscopic properties of
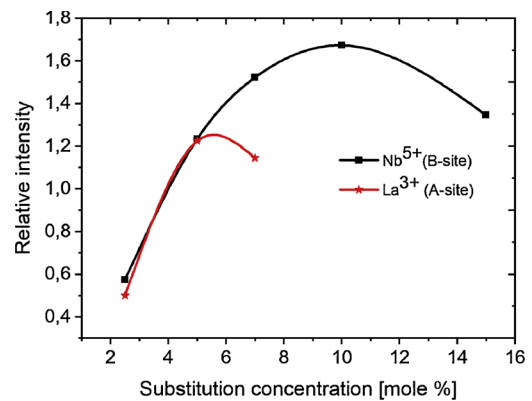

Fig. 3. Ratio of reduced relative intensity of mode 7 and mode 5. Note: 2.5% BLaT Raman intensities were adopted from Pokorny et al. [20].

BLaT samples, we ask the readers to refer to the available literature [20,21]. Mode 5 is a first-order Raman scattering mode that obeys the selection rules and is classified as symmetric octahedral breathing mode in the ferroelectric phase of BT. Initially, it is expected that the ratio of intensities should have a linear relationship because of the increase in vacancy concentration as a function of substitution. In Fig. 3, however, it can be seen that the relationship is clearly non-linear. It is important to understand that, at RT, FE is gradually lost in BNbT as the substitution concentration increases [24]. This can be due to various reasons, but in essence the material tends to become cubic with substitution concentration because of the discontinuity in the lattice continuum (breaking of O–Ti–O chains on the long range). The breaking of lattice continuity and loss of ferroelectricity in substituted systems can be found in detail in several reports [11,41,42]. The non-linear relationship obtained here is likely due to the gradual loss of polarizability of TiO_6 with substitution concentration coupled with the increase in the breathing mode of TiO_6 as a result of vacancies at the B-site. Non-linearity, in fact, starts to be obvious close to the substituent content corresponding to the loss of FE order in BNbT [24]. The same was repeated on BLaT since the two systems have same charge compensation mechanism although the substitution site is A-site in case of BLaT. A similar non-linear behaviour was observed in BLaT with a more pronounced non-linearity when the material is not FE anymore at RT [21]. The difference in the absolute value of relative intensities can be an indication that we have different degree of heterogeneity at the B-site in BNbT compared to BLaT. BNbT, in fact, may be more heterogeneous at the B-site than the BLaT since both $V_{Ti}^{''''}$ and Nb-substitution occur. These heterogeneities play a crucial role in defining phonon modes, so that disorder-related phonon modes become more pronounced in heterogeneous systems (i.e. less intense but broader Raman peaks).

4. Conclusion

The appearance of extra Raman modes in perovskites is directly related to lattice disorder and defects. Assigning these extra modes to a specific lattice vibration provides insight on modifications induced by chemical substitution in the material. Within this work, different perovskite $BaTiO_3$-based ceramics were fabricated to induce or suppress charge-compensating defects (i.e. B-site vacancies) in BT solid solutions, and were used as a basis to classify different kinds of extra Raman modes in the perovskite lattice. This work shows how defect-related modes can be classified as disorder-activated or localised modes in substituted BT perovskites. In particular, phonon modes originating from B-site vacancies in the perovskite lattice were elucidated, thus providing a straightforward methodology to quickly check the presence of this type of defects in substituted perovskites.

Declaration of Competing Interest

Acknowledgements

Appendix A. Supplementary data

Supplementary material related to this article can be found, in the online version, at doi:https://doi.org/10.1016/j.jeurceramsoc.2020.05.051.

References

[1] H.F. Kay, P. Vousden, XCV: Symmetry changes in barium titanate at low temperatures and their relation to its ferroelectric properties, London, Edinburgh, Dublin, Philos. Mag. J. Sci. 40 (1949) 1019–1040, https://doi.org/10.1080/14786444908561371.

[2] G.H. Kwei, A.C. Lawson, S.J.L. Billinge, S.W. Cheong, Structures of the ferroelectric phases of barium titanate, J. Phys. Chem. 97 (1993) 2368–2377, https://doi.org/10.1021/j100112a043.

[3] B. Jaffe, W. Cook, H. Jaffe, Piezoelectric Ceramics, Academic Press, London, 1971 https://cds.cern.ch/record/113309.

[4] G. Haertling, Ferroelectric ceramics: History and technology, J. Am. Ceram. Soc. 82 (1999) 718–818, https://doi.org/10.1111/j.1151-2916.1999.tb01840.x.

[5] H. Kishi, Y. Mizuno, H. Chazono, Base-metal electrode-multilayer ceramic capacitors: Past, present and future perspectives, Jpn. J. Appl. Phys. 42 (2003) 1–5, https://doi.org/10.1143/jjap.42.1.

[6] A. Matias, N. Nikola, R. Virginia, P. Satyanarayan, V. Rahul, K. Jurij, G.A. Rossetti Jr., R. Jürgen, BaTiO$_3$-based piezoelectrics: fundamentals, current status, and perspectives, Appl. Phys. Rev. 4 (2017) 1–53, https://doi.org/10.1063/1.4990046.

[7] A.K. Tagantsev, V.O. Sherman, K.F. Astafiev, J. Venkatesh, N. Setter, Ferroelectric materials for microwave tunable applications, J. Electroceram. 11 (2003) 5–66, https://doi.org/10.1023/B:JECR.0000015661.81386.e6.

[8] J. Rödel, W. Jo, K.T.P. Seifert, E.M. Anton, T. Granzow, D. Damjanovic, Perspective on the development of lead-free piezoceramics, J. Am. Ceram. Soc. 92 (2009) 1153–1177, https://doi.org/10.1111/j.1551-2916.2009.03061.x.

[9] T. Sluka, A.K. Tagantsev, D. Damjanovic, M. Gureev, N. Setter, Enhanced electromechanical response of ferroelectrics due to charged domain walls, Nat. Commun. 3 (2012) 748, https://doi.org/10.1038/ncomms1751.

[10] V.V. Shvartsman, D.C. Lupascu, Lead-free relaxor ferroelectrics, J. Am. Ceram. Soc. 95 (2012) 1–26, https://doi.org/10.1111/j.1551-2916.2011.04952.x.

[11] V.K. Veerapandiyan, M. Deluca, S.T. Misture, W.A. Schulze, S.M. Pilgrim, S.C. Tidrow, Dielectric and structural studies of ferroelectric phase evolution in dipole-pair substituted barium titanate ceramics, J. Am. Ceram. Soc. 103 (2020) 287–296, https://doi.org/10.1111/jace.16713.

[12] T. Maiti, R. Guo, A.S. Bhalla, Structure-property phase diagram of BaZr$_x$Ti$_{1-x}$O$_3$ system, J. Am. Ceram. Soc. 91 (2008) 1769–1780, https://doi.org/10.1111/j.1551-2916.2008.02442.x.

[13] R. Farhi, M. El Marssi, A. Simon, J. Ravez, Relaxor-like and spectroscopic properties of niobium modified barium titanate, Eur. Phys. J. B 18 (2000) 605–610, https://doi.org/10.1007/s100510070008.

[14] W. Kleemann, Random fields in relaxor ferroelectrics – A jubilee review, J. Adv. Dielectr. 2 (2012) 1241001, , https://doi.org/10.1142/S2010135X12410019.

[15] F.D. Morrison, A.M. Coats, D.C. Sinclair, A.R. West, Charge compensation mechanisms in La-doped BaTiO$_3$, J. Electroceram. 6 (2001) 219–232, https://doi.org/10.1023/A:1011400630449.

[16] R. Saito, M. Hofmann, G. Dresselhaus, A. Jorio, Advances in physics Raman spectroscopy of graphene and carbon nanotubes, Adv. Phys. 60 (2011) 413–550, https://doi.org/10.1080/00018732.2011.582251.

[17] E. Aksel, J.S. Forrester, B. Kowalski, M. Deluca, D. Damjanovic, J.L. Jones, Structure and properties of Fe-modified Na$_{0.5}$Bi$_{0.5}$TiO$_3$ at ambient and elevated temperature, Phys. Rev. B Condens. Matter Mater. Phys. 85 (2012) 21–24, https://doi.org/10.1103/PhysRevB.85.024121.

[18] V. Buscaglia, S. Tripathi, V. Petkov, M. Dapiaggi, M. Deluca, A. Gajović, Y. Ren,

[19] Average and local atomic-scale structure in BaZr$_x$Ti$_{1-x}$O$_3$ (x = 0.10, 0.20, 0.40) ceramics by high-energy x-ray diffraction and Raman spectroscopy, J. Phys. Condens. Matter 26 (2014) 065901, https://doi.org/10.1088/0953-8984/26/6/065901.

[19] M.P. Fontana, M. Lambert, Linear disorder and temperature dependence of Raman scattering in BaTiO$_3$, Solid State Commun. 10 (1972) 1–4, https://doi.org/10.1016/0038-1098(72)90334-1.

[20] J. Pokorný, U.M. Pasha, L. Ben, O.P. Thakur, D.C. Sinclair, I.M. Reaney, Use of Raman spectroscopy to determine the site occupancy of dopants in BaTiO$_3$, J. Appl. Phys. 109 (2011), https://doi.org/10.1063/1.3592192.

[21] F.D. Morrison, D.C. Sinclair, J.M.S. Skakle, A.R. West, Very-high-permittivity barium titanate ceramics, J. Am. Ceram. Soc. 60 (1998) 1957–1960.

[22] A. Feteira, D.C. Sinclair, I.M. Reaney, M.T. Lanagan, Structure-property relationships of BaTi$_{1-2y}$Ga$_y$Nb$_y$O$_3$ (0 < =y < =0.35) ceramics, J. Am. Ceram. Soc. 88 (2005) 3055–3062, https://doi.org/10.1111/j.1551-2916.2005.00580.x.

[23] F.D. Morrison, D.C. Sinclair, A.R. West, Electrical and structural characteristics of lanthanum-doped barium titanate ceramics, J. Appl. Phys. 86 (1999) 6355–6366, https://doi.org/10.1063/1.371698.

[24] R. Farhi, M. El Marssi, A. Simon, J. Ravez, Relaxor-like and spectroscopic properties of niobium modified barium titanate, Eur. Phys. J. B 18 (2000) 605–610, https://doi.org/10.1007/s100510070008.

[25] M. DiDomenico, S.H. Wemple, S.P.S. Porto, R.P. Bauman, Raman spectrum of single-domain BaTiO$_3$, Phys. Rev. Lett. 174 (1968) 522–530, https://doi.org/10.1103/PhysRevLett.78.2397.

[26] D. Schütz, M. Deluca, W. Krauss, A. Feteira, T. Jackson, K. Reichmann, Lone-pair-induced covalency as the cause of temperature- and field-induced instabilities in bismuth sodium titanate, Adv. Funct. Mater. 22 (2012) 2285–2294, https://doi.org/10.1002/adfm.201102758.

[27] A. Slodczyk, P. Colomban, Probing the nanodomain origin and phase transition mechanisms in (un) poled PMN-PT single crystals and textured ceramics, Mater. (Basel) 3 (2010) 5007–5028.

[28] C.W. Ahn, C.H. Hong, B.Y. Choi, H.P. Kim, H.S. Han, Y. Hwang, W. Jo, K. Wang, J.F. Li, J.S. Lee, I.W. Kim, A brief review on relaxor ferroelectrics and selected issues in lead-free relaxors, J. Korean Phys. Soc. 68 (2016) 1481–1494, https://doi.org/10.3938/jkps.68.1481.

[29] R. Farhi, M. El Marssi, J.L. Dellis, Y.I. Yuzyuk, J. Ravez, M.D. Glinchuk, Raman scattering from relaxor ferroelectrics and related compounds, Ferroelectrics 235 (1999) 9–17, https://doi.org/10.1080/00150199908214863.

[30] H.M. Jang, T. Kim, I. Park, Nano-sized polar clusters with tetragonal symmetry in PbTiO$_3$-based relaxor ferroelectrics, Solid State Commun. 127 (2003) 645–648, https://doi.org/10.1016/S0038-1098(03)00564-7.

[31] M. Deluca, G. Picht, M.J. Hoffmann, A. Rechtenbach, J. Töpfer, F.H. Schader, K.G. Webber, Chemical and structural effects on the high-temperature mechanical behavior of (1-x) (Na$_{1/2}$Bi$_{1/2}$)TiO$_3$-xBaTiO$_3$ ceramics, J. Appl. Phys. 117 (2015), https://doi.org/10.1063/1.4916784.

[32] M. Deluca, Z.G. Al-Jlaihawi, K. Reichmann, A.M.T. Bell, A. Feteira, Remarkable impact of low BiYbO$_3$ doping levels on the local structure and phase transitions of BaTiO$_3$, J. Mater. Chem. A Mater. Energy Sustain. 6 (2018) 5443–5451, https://doi.org/10.1039/c7ta11096k.

[33] D.A. Tenne, I.E. Gonenli, A. Soukiassian, D.G. Schlom, S.M. Nakhmanson, K.M. Rabe, X.X. Xi, Raman study of oxygen reduced and re-oxidized strontium titanate, Phys. Rev. B 76 (2007) 024303, https://doi.org/10.1103/PhysRevB.76.024303.

[34] H. Harima, Properties of GaN and related compounds studied by means of Raman scattering, J. Phys. Condens. Matter 14 (2002) R967–R993, https://doi.org/10.1088/0953-8984/14/38/201.

[35] S. Nakashima, H. Harima, Characterization of Defects in SiC Crystals by Raman Scattering, (2004), pp. 585–605, https://doi.org/10.1007/978-3-642-18870-124.

[36] T. Wu, J. Lin, Transition of compensating defect mode in niobium-doped barium titanate, J. Am. Ceram. Soc. 77 (1994) 759–764, https://doi.org/10.1111/j.1151-2916.1994.tb05362.x.

[37] F.J. Crowne, S.C. Tidrow, D.M. Potrepka, A. Tauber, Microfields induced by random compensated charge pairs in ferroelectric materials, MRS Proc. 720 (2002), https://doi.org/10.1557/PROC-720-H5.1 H5.1..

[38] S. Wada, T. Suzuki, M. Osada, M. Kakihana, T. Noma, Change of macroscopic and microscopic symmetry of barium titanate single crystal around curie temperature, Jpn. J. Appl. Phys. 37 (1998) 5385–5393, https://doi.org/10.1143/JJAP.37.5385.

[39] R. Farhi, M. El Marssi, A. Simon, J. Ravez, A Raman and dielectric study of ferroelectric ceramics, Eur. Phys. J. B 9 (1999) 599–604, https://doi.org/10.1007/s100510050803.

[40] D. Chapron, F. Cordero, M.D. Fontana, Characterization of oxygen vacancies in SrTiO$_3$ by means of anelastic and Raman spectroscopy, J. Appl. Phys. 126 (2019) 154101, https://doi.org/10.1063/1.5115106.

[41] G. Canu, G. Confalonieri, M. Deluca, L. Curecheriu, M.T. Buscaglia, M. Asandulesa, N. Horchidan, M. Dapiaggi, L. Mitoseriu, V. Buscaglia, Structure-property correlations and origin of relaxor behaviour in BaCe$_x$Ti$_{1-x}$O$_3$, Acta Mater. 152 (2018), https://doi.org/10.1016/j.actamat.2018.04.038.

[42] A.A. Bokov, Z.-G.Z.-G. Ye, Recent progress in relaxor ferroelectrics with perovskite structure, J. Mater. Sci. 41 (2006) 31–52, https://doi.org/10.1007/s10853-005-5915-7.